Supplementary materials

Comprehensive Study of Li^{+}/Ni^{2+} Disorder in Ni-Rich NMCs Cathodes for Li-Ion Batteries

Elena D. Orlova [1], Aleksandra A. Savina [1,*], Sergey A. Abakumov [2], Anatolii V. Morozov [1] and Artem M. Abakumov [1]

[1] Center for Energy Science and Technology, Skolkovo Institute of Science and Technology, Nobel Str. 3, 121205 Moscow, Russia; Elena.Orlova2@skoltech.ru (E.D.O.); Anatolii.Morozov@skoltech.ru (A.V.M.); A.Abakumov@skoltech.ru (A.M.A.)

[2] Laboratory for Molecular Imaging and Photonics, KU Leuven, Celestijnenlaan 200F, B-3001 Leuven, Belgium; sergey.abakumov@kuleuven.be

* Correspondence: A.Savina@skoltech.ru; Tel.: +79-246571299

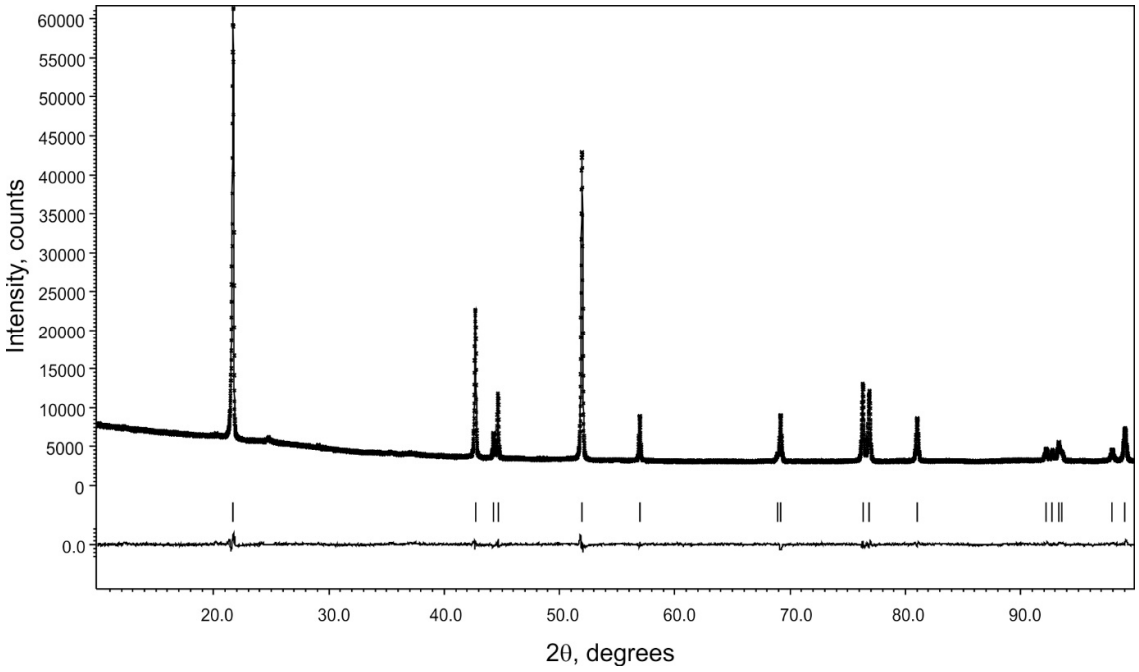


Figure S1. Experimental, calculated and difference PXRD profiles after the Rietveld refinement of the NMC811 structure in the S1air sample. Vertical bars indicate Bragg reflection positions.

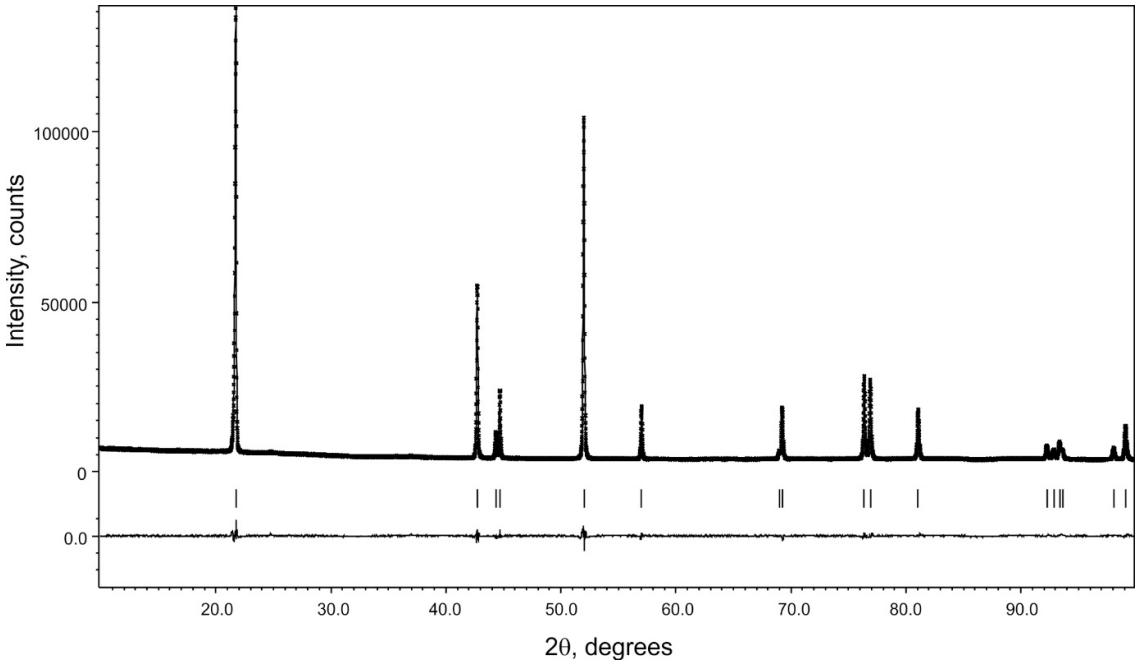


Figure S2. Experimental, calculated and difference PXRD profiles after the Rietveld refinement of the NMC811 structure in the S2air sample. Vertical bars indicate Bragg reflection positions.

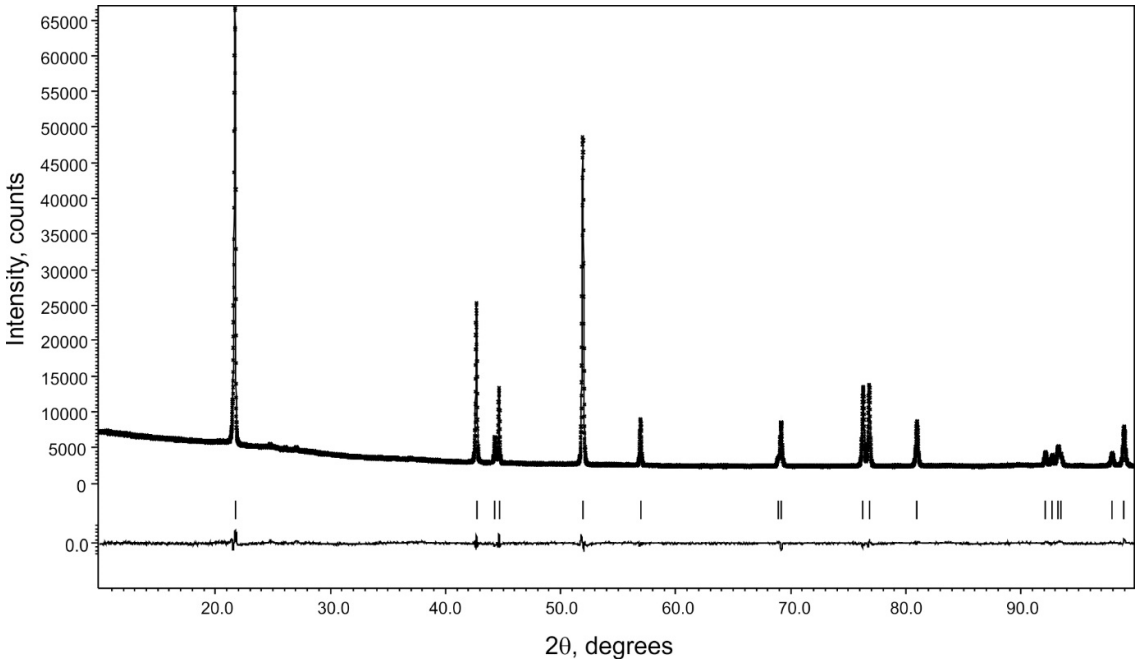


Figure S3. Experimental, calculated and difference PXRD profiles after the Rietveld refinement of the NMC811 structure in the S3air sample. Vertical bars indicate Bragg reflection positions.

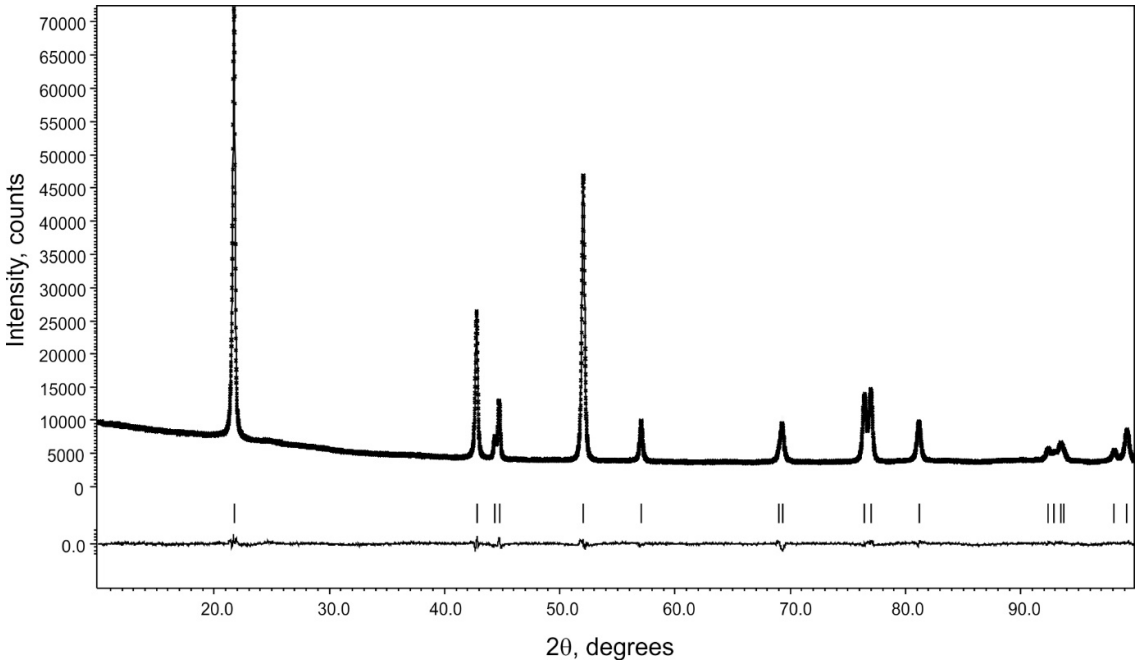


Figure S4. Experimental, calculated and difference PXRD profiles after the Rietveld refinement of the NMC811 structure in the S1ox sample. Vertical bars indicate Bragg reflection positions.

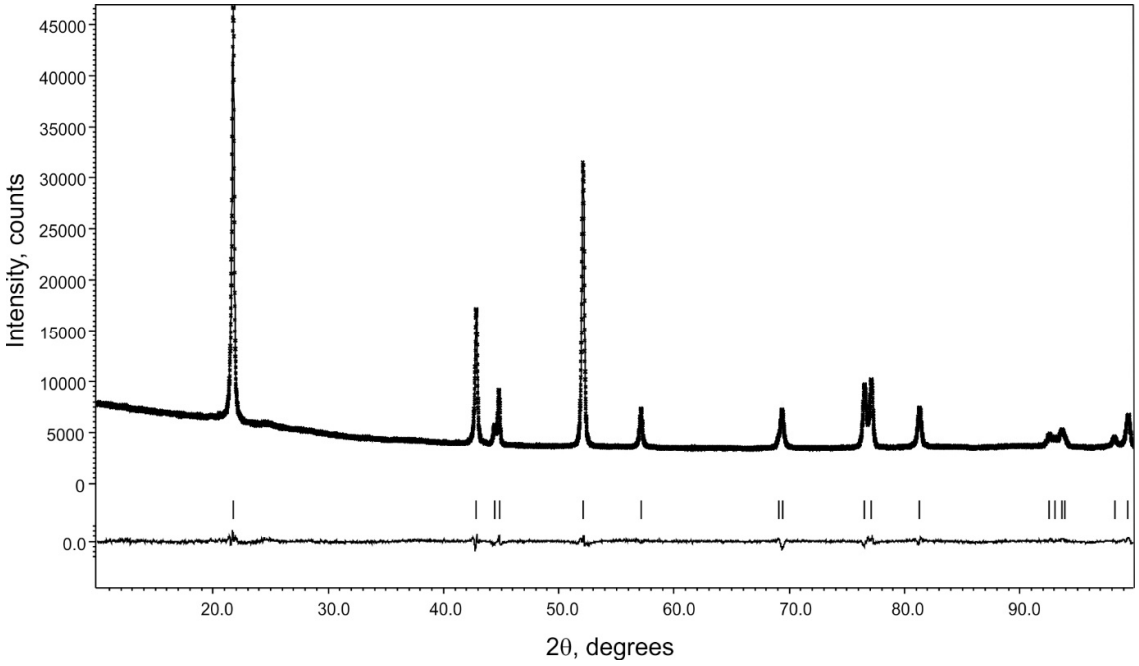


Figure S5. Experimental, calculated and difference PXRD profiles after the Rietveld refinement of the NMC811 structure in the S2ox sample. Vertical bars indicate Bragg reflection positions.

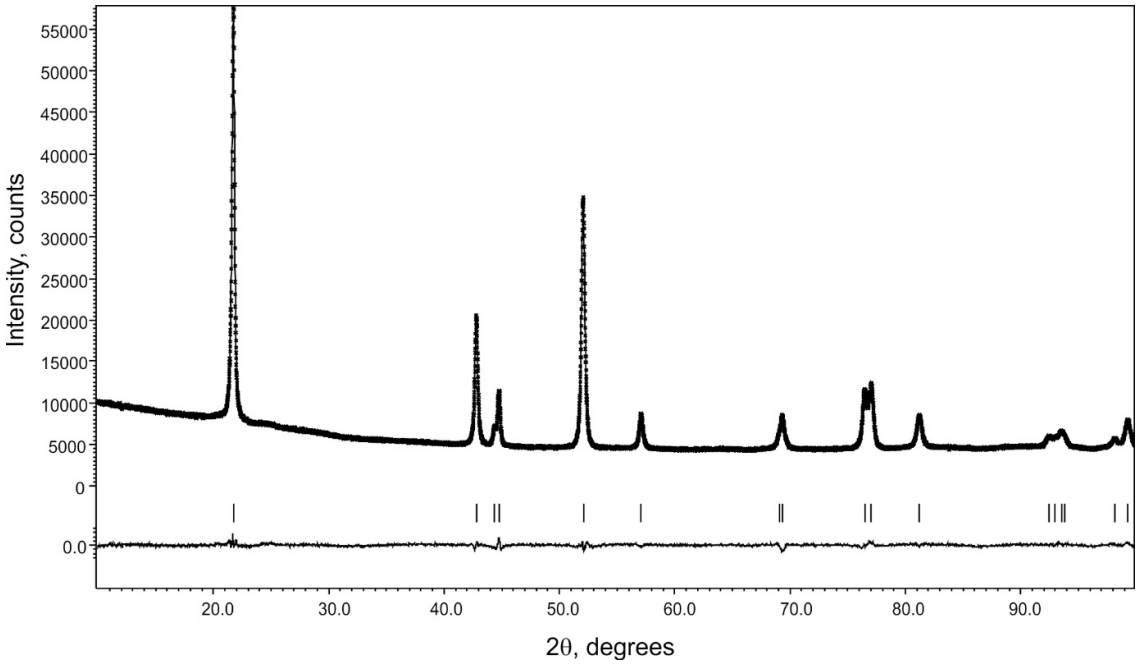


Figure S6. Experimental, calculated and difference PXRD profiles after the Rietveld refinement of the NMC811 structure in the S3ox sample. Vertical bars indicate Bragg reflection positions.

Table S1. Results of the 3D-ED study of Ni^{2+}/Li^{+} anti-site defects

Sample	Acquisition angular range, degrees	Refined composition	Ni^{2+} in Li site, %	Li^{+} in Ni site, %	$max\ \frac{Sin\ \theta}{\lambda}$	Number of independent reflections	R_F, %
S1air							
Crystal 1	-45 - +45	$Li_{0.951}Ni_{0.830}Mn_{0.1}Co_{0.1}O_2$	3.36(5)	0	0.525	18	31.9
Crystal 2	-40 - +43	$Li_{0.869}Ni_{0.829}Mn_{0.1}Co_{0.1}O_2$	3.24(9)	0	0.704	29	23.8
Crystal 3	-45 - +45	$Li_{0.953}Ni_{0.839}Mn_{0.1}Co_{0.1}O_2$	3.45(6)	0	0.525	18	28.7
S2air							
Crystal 1	-45 - +45	$Li_{0.977}Ni_{0.824}Mn_{0.1}Co_{0.1}O_2$	2.43(4)	0	0.538	19	22.9
Crystal 2	-45 - +45	$Li_{0.98}Ni_{0.821}Mn_{0.1}Co_{0.1}O_2$	2.51(5)	0	0.435	20	21.0
Crystal 3	-45 - +40	$Li_{0.977}Ni_{0.823}Mn_{0.1}Co_{0.1}O_2$	2.36(4)	0	0.549	18	29.9
S3air							
Crystal 1	-43 - +43	$Li_{0.977}Ni_{0.863}Mn_{0.1}Co_{0.1}O_2$	5.78(4)	0	0.681	29	24.6
Crystal 2	-45 - +39	$Li_{0.878}Ni_{0.863}Mn_{0.1}Co_{0.1}O_2$	6.12(6)	0	0.526	19	20.6
Crystal 3	-44 - +43	$Li_{0.949}Ni_{0.852}Mn_{0.1}Co_{0.1}O_2$	5.34(7)	0	0.683	23	24.1
S1ox							
Crystal 1	-41 - +38	$Li_{1.017}Ni_{0.823}Mn_{0.1}Co_{0.1}O_2$	2.24(6)	1.97(1)	0.706	28	18.3
Crystal 2	-41 - +42	$Li_{0.997}Ni_{0.823}Mn_{0.1}Co_{0.1}O_2$	2.64(5)	1.38(8)	0.679	28	27.2
Crystal 3	-45 - +45	$Li_{1.014}Ni_{0.827}Mn_{0.1}Co_{0.1}O_2$	2.71(4)	2.09(4)	0.525	18	22.3
S2ox							
Crystal 1	-45 - +41	$Li_{1.015}Ni_{0.824}Mn_{0.1}Co_{0.1}O_2$	2.44(3)	1.95(6)	0.514	26	24.7
Crystal 2	-47 - +42	$Li_{1.015}Ni_{0.830}Mn_{0.1}Co_{0.1}O_2$	2.34(7)	1.79(5)	0.442	18	21.9
Crystal 3	-45 - +37	$Li_{1.017}Ni_{0.823}Mn_{0.1}Co_{0.1}O_2$	2.21(6)	1.89(7)	0.531	25	19.7
S3ox							
Crystal 1	-45 - +45	$Li_{1.011}Ni_{0.830}Mn_{0.1}Co_{0.1}O_2$	2.71(6)	1.77(8)	0.510	20	18.9
Crystal 2	-45 - +45	$Li_{1.012}Ni_{0.828}Mn_{0.1}Co_{0.1}O_2$	2.73(8)	1.89(8)	0.521	19	14.3
Crystal 3	-45 - +45	$Li_{1.009}Ni_{0.831}Mn_{0.1}Co_{0.1}O_2$	2.68(4)	1.62(8)	0.524	18	27.0

Clusterization procedure.

In order to perform clusterization the images were Fourier-transformed first and oriented with respect to the internal coordinate system by aligning the 00l reciprocal lattice row along the x-axis. The atom counts along the layers of the 3*a* and 3*b* sites are then projected onto the y-axis, yielding an alternating pattern of peaks, with less intense peaks corresponding to the Ni cations located in the Li 3*a* sites. The exact location of each peak is determined by MATLAB's built-in function. Once the positions of the rows along the y-axis have been found, the atom x-y positions are assigned to either 3*a* or 3*b* atomic columns. In present work, "cluster" is defined not as a lattice unit cell, but as a parallelogram, where the 3*b* atomic columns are located at the vertices with the 3*a* atomic column at the center. It was assumed that the crystal thickness within one cluster remains the same, since the projected distance between the most distant points in the cluster does not exceed 5 Å. The assignment of atomic columns, belonging to each cluster, was conducted by determining the Euclidean distance between them and finding the closest neighbors. Thus, each five columns (four for the 3*b* positions and one for the 3*a* position) were considered as a "cluster" with the atom counts normalized to the number of respective columns. In that way, each "cluster" was marked with certain color in accordance with colorbar, corresponding to the relative concentration of the Ni ions ($\frac{N_{3a}}{N_{3a}+N_{3b}}$) within one cluster cell, which could rewritten in terms of occupancy factors in the following manner $\frac{g(Ni)_{3a}}{g(Ni)_{3a}+g(Ni)_{3b}}$ assuming equal total number of sites in the atomic columns of each cluster due to constant thickness.